

## Phase Behavior and Network Formation in a Cationic Surfactant-Fatty Alcohol-Water System

William J. Benton<sup>a,1</sup>, Clarence A. Miller<sup>a</sup> and Robert L. Wells<sup>b</sup>

<sup>a</sup>Department of Chemical Engineering, Rice University, PO Box 1892, Houston, Texas 77251, and <sup>b</sup>Procter and Gamble Company, Sharon Woods Technical Center, Cincinnati, Ohio.

Optical microscopy and differential scanning calorimetry were used to study the behavior of dilute aqueous systems containing mixtures of a long-chain cationic surfactant and long-chain fatty alcohols. Both alcohol-rich particles with a lamellar structure and crystalline fibers containing considerable surfactant were observed, the fibers becoming more prevalent with decreasing values of the alcohol-to-surfactant ratio  $r$ . For values of  $r$  exceeding about two, separate fibrous and particulate regions were seen, the latter forming continuous networks throughout individual samples and hence contributing to the viscoelastic properties known to characterize these formulations. Studies of system behavior as a function of temperature showed that melting temperatures of the fibers and particles were about 55 C and 60 C, respectively.

The phase behavior of surfactant-alcohol-water systems is complex. In many such systems various liquid, liquid crystalline and solid phases are found. The liquids, especially those containing micelles, and liquid crystalline phases have been the subject of considerable research in recent years which has led to an improved understanding of their internal structure and properties (1-4). Much less is known about the solid phases, however.

Nevertheless, solid phases occur in some systems of practical importance. The present study, for instance, focuses on a system containing a long-chain cationic surfactant and a mixture of long-chain fatty alcohols. Similar systems have been the subject of several previous studies (5-8) because of their use in various waxes, cosmetics, personal care products and pharmaceutical preparations.

Of particular interest here is the suggestion made in these papers that particles of a surfactant-rich phase can sometimes form a network structure which imparts viscoelastic properties to even quite dilute formulations of this type, i.e., those containing over 90% water. Indeed, Gstirner et al. (9) observed with electron microscopy a network consisting of interlocked chains of submicroscopic particles (0.1-1 $\mu$ m diameter) in a closely related system containing a mixture of long-chain anionic surfactants and long-chain fatty alcohols. The particles appeared to be of more or less spherical shape. In all these studies of network development attention was limited to systems with a high ratio of fatty alcohol to surfactant, approximately 9:1 by weight.

The formation of networks in dilute colloidal dispersions is not, of course, limited to surfactant-containing

systems. Overbeek (10,11) has suggested that networks can form in dispersions where the particles are highly anisotropic or attract one another strongly. Figure 1 is a schematic view of such a network, the cells being water enclosed by a continuous thin layer of closely-spaced particles. A possible mechanism of network formation involving spinodal decomposition has been put forward recently and a theoretical analysis presented for the case of strongly interacting spherical particles (12).

The existence of a network structure is also related to syneresis, the release of water from a viscoelastic preparation. When a structure such as that of Figure 1 is disturbed, for example by being sheared, the network is broken at certain points. Since the interaction between particles is attractive, the network has a tendency to become more compact so that excess water is exuded. These changes in network structure also produce changes in rheological properties such as a yield point and shear-dependent viscosity.

The objective of the present study was to determine by optical microscopy and differential scanning calorimetry the phase behavior and microstructure on the colloidal scale of a cationic surfactant-fatty alcohol-water system as a function of composition and temperature. As discussed below, the observations reveal that two types of colloidal particles can form in

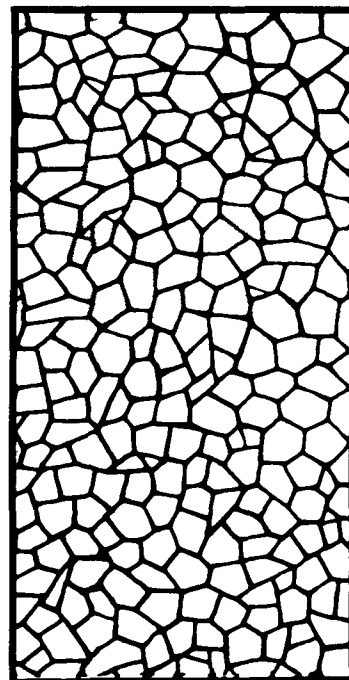


FIG. 1. Network formation in unstable colloidal suspension.

<sup>1</sup>Now with Standard Oil Co. Research Center, 4440 Warrensville Center Rd., Cleveland, Ohio 44128-2837.

this system. They also confirm that a network does develop under some circumstances and provide information about its structure.

## EXPERIMENTAL

The surfactant used in the experiments was Stedbac (stearyl dimethyl benzyl ammonium chloride), manufactured by Hexcel, Inc. (Zeeland, Michigan). A 60:40 mixture by weight of cetyl and stearyl alcohols was used because it is the eutectic composition and thus minimizes the likelihood of alcohol recrystallization at low temperatures (13). The individual fatty alcohols (FA) were provided by the Procter and Gamble Company (CO-1695 and CO-1897) and had purities of 95% and 97%, respectively. The water was deionized and distilled (Ricca, Inc., Dallas, Texas).

Appropriate quantities of the two solid alcohols for a 60:40 mixture were combined, heated above the melting point (to about 70 C), and mixed thoroughly with a magnetic stirrer. The FA melt was then poured into a glass vial, allowed to recrystallize, and stored at room temperature.

Weighed amounts of Stedbac and of the FA mixture were combined with the correct volumes of distilled water to form 10-g samples in Teflon-capped flat-bottomed test tubes. The samples were heated to 50 C, where the Stedbac dissolved and the FA crystals floated to the top of the aqueous phase. The solutions were further heated until the FA mixture melted. Thorough mixing was achieved by several heating and cooling cycles with frequent vortex mixing. This procedure required three or four days. Once relatively homogeneous and uniform mixtures were formed, they were stored in an environmental room maintained at  $30.0 \pm 0.5$  C.

After storage for a suitable time, the test tubes were viewed when placed between two sheets of polarizing material having perpendicular orientations (14,15). The textures and any phase separation observed with this polarized light screening (PLS) technique were noted for various samples with different compositions.

Rectangular optical capillaries (Vitro Dynamics, Inc., Rockaway, New Jersey) having an optical pathwidth of 100  $\mu$ m were used for the microscopy studies (16). Samples were imbibed by capillary action, either shortly after mixing or after storage at constant temperature for an extended period. Once a sufficient volume of the mixture was imbibed into the capillaries, they were sealed with a fast-setting, two-part epoxy resin and fastened to standard microscope slides for ease in handling. Owing to the high viscosity of some samples, it took several hours to several days to fill a reasonable volume of the cell by capillary action.

A Nikon polarizing microscope (Optiphot-Pol) was used. It was equipped with a 35-mm camera and an automatic exposure control system (Nikon UFX). Selected samples were examined by both conventional polarizing microscopy and with modulation contrast optics (17), a filtering system which enhances variations in optical density and hence enables structural details to be discerned. Modulation contrast optics have been used previously to study the defect structure in lamellar liquid crystals (18). A Mettler hot stage (FP52)

and controller (FP5) were used to investigate temperature effects.

Differential scanning calorimetry (DSC) studies were made on samples having various ratios of a FA mixture to Stedbac. The FA mixture for the DSC studies was 50/50 wt % cetyl/stearyl. The measurements were made on a Perkin Elmer DSC-2C at a heating rate of 10 C/min. For the water-free studies, the proper proportions of this FA mixture and Stedbac were melted together and held at about 80 C until clear, cooled to room temperature and held there for 24 hr before sampling for DSC measurement. For aqueous systems the water was heated to 80 C, the Stedbac added and stirred until clear, and then the FA added. The mixture was stirred for about 10 min, then cooled while stirring. It was reheated to 80 C and cooled while stirring one more time, then held 24 hr at room temperature before sampling for DSC.

## RESULTS

*Composition effects on phase behavior in Stedbac-water-fatty alcohol systems.* The polarized light screening (PLS) technique was used to observe the behavior of various samples containing water, Stedbac and the FA mixture at 30 C. More than 100 samples were viewed, with the Stedbac concentration ranging between 0 and 2 wt % and the FA concentration between 0 and 6 wt %. Relatively few samples were formulated in the regions exhibiting macroscopic phase separation (see below) and for alcohol contents above 3 wt %. All samples were allowed to equilibrate for at least 60 days at  $30.0 \pm 0.5$  C.

As indicated in Figure 2, macroscopic phase separation into a colloidal dispersion exhibiting some birefringence and an isotropic aqueous phase was observed when surfactant content was below 0.3 wt % and FA content below about 3 wt %. Separation also was seen at higher surfactant contents whenever the alcohol-to-surfactant ratio dropped below about 0.9. Since compositions exhibiting such separation are not of practical interest, this region was not studied further.

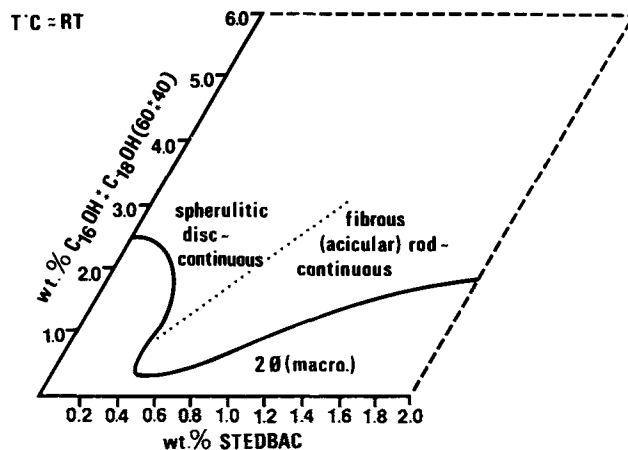
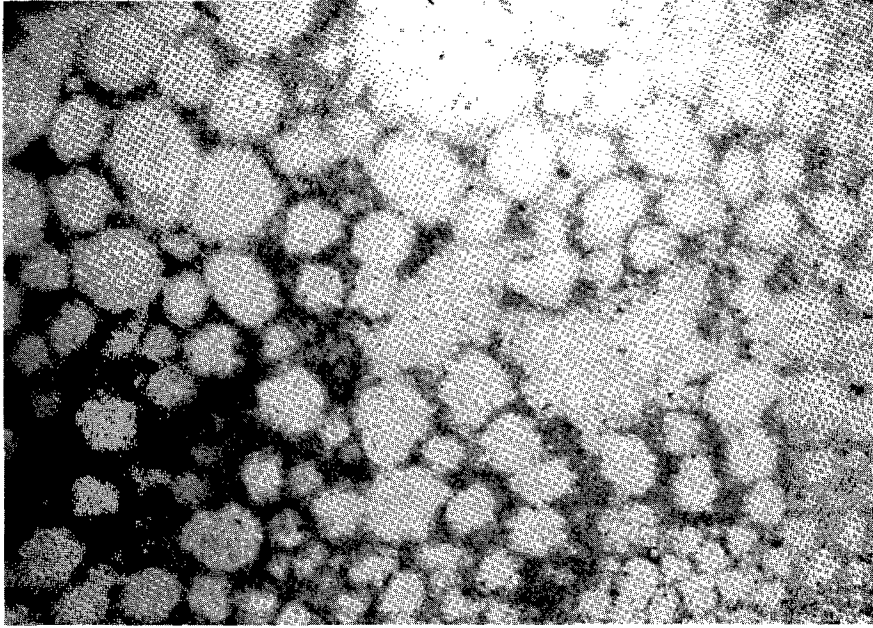
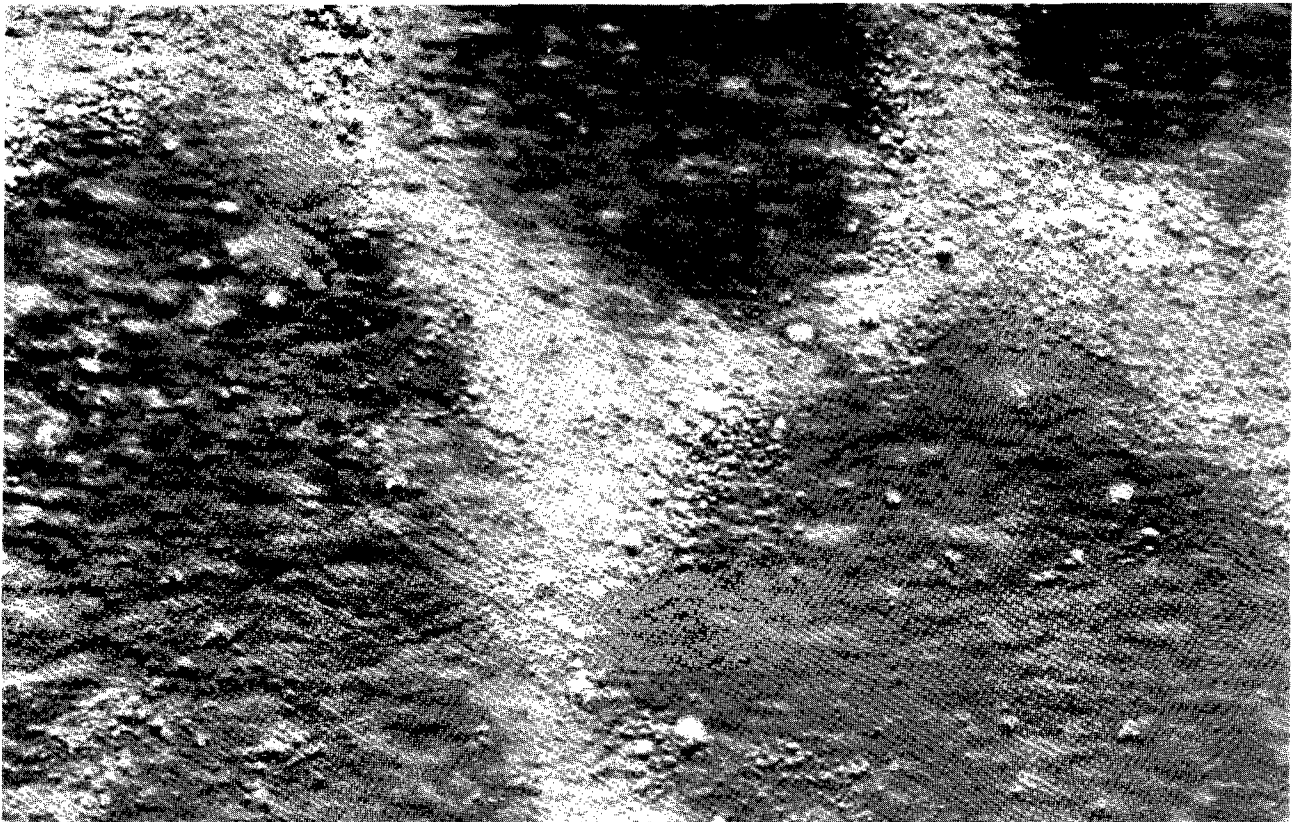


FIG. 2. Schematic phase diagram from microscopy at room temperature of Stedbac and  $C_{16}OH$ :  $C_{18}OH$  (60:40) mixture.



**FIG. 3. Photomicrograph of 0.4% Stedbac and 2.1% FA mix. Pol +  $1/4\lambda$ .  $\times 72$ .**



**FIG. 4. Photomicrograph of 0.4% Stedbac and 2.1% FA mix. Modulation contrast  $\times 361$ .**

## PHASE BEHAVIOR AND NETWORK FORMATION

At other compositions no macroscopic phase separation occurred. The samples in the low FA portion of this region exhibited some birefringence, while those with higher FA contents scattered light extensively and appeared creamy. As discussed below, these samples also contained birefringent material, but the birefringence was obscured by scattering during the macroscopic (PLS) observations.

Optical microscopy was used to observe at room temperature a series of samples containing 2.1 and 3.0 wt % of the FA mixture, with Stedbac concentrations ranging from 0.4 to 1.2 wt % in each case. The use of modulation contrast optics was emphasized because it provided a clearer picture of system structure.

Figure 3 shows that at the lowest surfactant



FIG. 5. Photomicrograph of 0.4% Stedbac and 2.1% FA mix. Modulation contrast  $\times 723$ .

concentration of 0.4 wt %, many small particles are present. When viewed with crossed polarizers, these particles exhibit Maltese crosses. They appear generally spherical with sizes below about 10  $\mu\text{m}$ . But they may well be disk-like, as we have found for particles of similar appearance in systems containing anionic surfactants and short-chain alcohols (19) and as others have also reported (20). Although Figure 3 is for a sample containing 2.1 wt % FA, similar behavior was seen when the FA concentration was raised to 3.0 wt %.

Particularly striking in Figure 3 is the nonuniform distribution of particles. Indeed, numerous regions having dimensions of about 100  $\mu\text{m}$  appear to be virtually free of particles. However, careful inspection of Figure 4, taken at higher magnification, reveals that the "particle-free" regions contain many closely-spaced fibrous crystals. At still higher magnification the particle-containing regions are found to themselves have small patches of fibrous material where particles are excluded (Fig. 5). We emphasize that division of the sample into particulate and fibrous regions is on a microscopic scale only. No macroscopic phase separation was seen in the test tubes having the same overall compositions, even after extended storage for several months.

Returning to Figures 3 and 4, we note that the particle-containing regions are interconnected and appear to extend throughout the entire sample. This conclusion has been confirmed by focusing at different depths to follow the particle-rich regions over long distances. Thus, these regions form a network which may impart viscoelastic properties to the overall

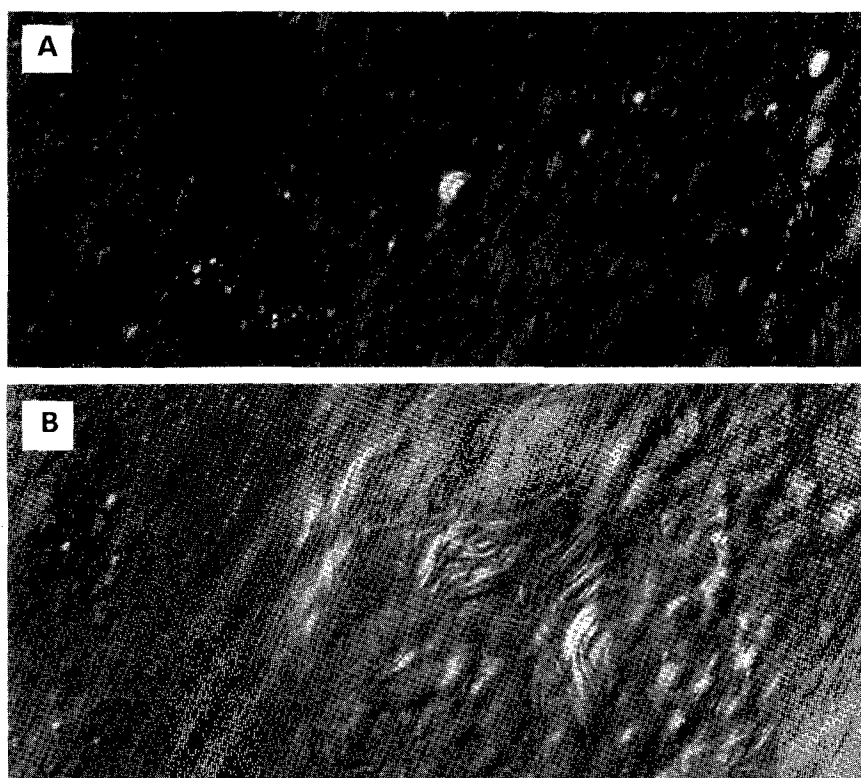


FIG. 6. Photomicrograph of 1.0% Stedbac and 2.1% FA mix. Modulation contrast  $\times 723$ . (A) Fibrous region with some particles; (B) fibrous region with no particles.

mixture similar to those which have been found in closely-related systems (5-8). The two-dimensional view of Figure 3 suggests that the fibrous regions are largely isolated. It is conceivable, however, that interconnections would be found upon careful investigation of the three-dimensional structure. In any case the existence of the microscopic network structure leads to high stability with respect to macroscopic phase separation exhibited by these dilute formulations.

With FA content maintained constant at 2.1%, separation into microscopic fibrous and particulate regions as described above was seen at concentrations of 0.4% and 0.6% Stedbac. As surfactant concentration increased, fewer particles and more fibers were visible. At 1.0% surfactant the relatively few particles present were incorporated within the fibrous regions as shown in Figure 6A, i.e., there were no separate particulate regions. Other parts of the fibrous regions remained largely free of particles and exhibited greater overall alignment (Fig. 6B). As shown in Figure 6B, some microscopic separation was again observed, but in this case the fibrous regions evidently coexisted with domains of the continuous aqueous phase. A few particles exhibiting Brownian motion could be seen in the aqueous regions. It appears from large-scale views of other samples containing many fibers and few particles that the fibrous regions can sometimes form networks. If so, it seems likely that such networks, which contain significant amounts of nearly particle-free water, would be more susceptible to structural breakdown and syneresis than those discussed above where no large, separated aqueous domains exist.

At 1.2% Stedbac even fewer particles are present. Figure 7 shows that fibrous crystals can form around a particle, giving its external boundary a polygonal appearance, generally hexagonal. As indicated below, the FA-rich particles form first on cooling, and their surfaces may provide sites for nucleation and growth of the fibrous crystals at lower temperatures. Also visible in the upper righthand corner of Figure 7 is part of an aqueous region which has separated as described above.

A similar study was made of the effect of surfactant concentration with FA concentration maintained constant at 3%. As mentioned previously, network formation and separate particulate and fibrous regions

were observed at low surfactant concentrations (Fig. 4). As surfactant concentration increased, there were again fewer particles and more fibers, although at a given surfactant concentration more particles were present at 3% FA than at 2.1% FA. The few particles present at a surfactant concentration of 1.4% were again incorporated into the fibrous regions. But no separation of aqueous regions was observed at 3% FA. The mixtures had a rather uniform appearance similar to that of Figure 6A and were quite viscous. At 2.0% surfactant there was even more fibrous material, and some of it collected in small globular domains which seemed to aggregate to form larger clumps.

Figure 2 provides an overall summary of the microscopy results for samples containing no more than 3 wt % alcohol. The boundary between compositions having a network of separate particulate and fibrous regions and compositions having only fibrous regions is not sharp but occurs at an FA-to-Stedbac ratio of about two on a weight basis, the ratio increasing slightly with increasing FA content.



FIG. 7. Photomicrograph of 1.2% Stedbac and 2.1% FA mix. Modulation contrast  $\times 800$ .

TABLE 1

Endotherms of Anhydrous FA-Stedbac Systems

Wt % FA	Wt % Stedbac	Endotherms [onset temp., °C (enthalpy, cal/g)]		
		T <sub>1</sub>	T <sub>2</sub>	T <sub>3</sub>
100	0	25 ( 6)	51 (32)	—
90	10	19 ( 6)	52 (24)	61 ( 3)
67	33	—	50 ( 7)	71 (25)
50	50	—	—	78 (33)
40	60	—	48 ( 1.4)	71 (25)
20	80	14 ( .7)	42 ( 4)	59 (14)
10	90	17 (10)	41 ( .9)	60 ( 2.5)
0	100	—	—	64 (33)

## PHASE BEHAVIOR AND NETWORK FORMATION

**DSC results.** DSC studies were first done on Stedbac-FA mixtures without added water. Table 1 shows the onset temperatures and enthalpies of the endotherms found for samples of varying Stedbac and FA concentrations. The enthalpies are expressed in cal/g of total sample, so they do not necessarily express the absolute enthalpy of the transition except when the entire sample is participating in the particular phase change. If the actual enthalpy changes for two peaks are similar (e.g.,  $T_2$  and  $T_3$ ), then the size of the measured enthalpy change for a peak may indicate approximately the amount of the sample participating in that phase change. We note further that the observed transitions are not isothermal. The results likely depend on heating and cooling rates to some extent because of molecular transport processes which occur in addition to the actual phase transformations.

For the pure fatty alcohol mixture we obtain results in good agreement with those of Kolp and Lutton (21) (Fig. 8A). The lower peak is the change from  $\beta$  to  $\alpha$  crystalline forms while the peak at 51 C is the melting point of this mixture. With addition of 10% Stedbac these two peaks are still present but diminished in size while a new high temperature peak has appeared. The lower peaks gradually disappear and the amount of material participating in the higher temperature peak increases as the amount of Stedbac is increased to 50%.

The trends of peak sizes in the region of 0 to 50% Stedbac suggest strongly that two different crystals exist in this composition range. One melts at about 51 C, contains very little Stedbac and is predominant at high FA/Stedbac ratios. The other melts at about 78 C, contains about equal amounts of FA and Stedbac on a weight basis and is predominant at higher surfactant concentrations (Fig. 8B). The data also suggest that this system has a eutectic temperature of about 50 C.

At approximately 100% Stedbac (a small amount of water is probably present since the material was not dried) there is a transition at 64 C from crystal to lamellar liquid crystal (Fig. 8C). In the Stedbac/water phase diagram shown in Figure 9 the lamellar region continues down to about 85% Stedbac. A viscous isotropic phase and a hexagonal phase are found at lower Stedbac concentrations. Note that even in dilute aqueous systems Stedbac crystals are found at temperatures below about 40 C.

With addition of water to 50%, the DSC results show that the FA melting peak at about 50 C is lost and all the material melts at a higher temperature, as shown in Table 2. In this table, the enthalpies are based on the total solids weight (FA + Stedbac) in the sample excluding the water, even though some water may be in the dispersed phase and a small amount of Stedbac is dissolved in the water.

At even higher water levels a peak is found in the mid-50's, in addition to the high temperature peak. From the DSC studies alone, it is not clear whether the two different crystals seen in anhydrous systems also exist at high water levels. The tradeoff in size of one peak for another on the repeat heating of the high water 91/9 sample suggests that the two peaks are melting points of different crystals instead of the same material undergoing two sequential phase transitions, as in the pure fatty alcohol. Indeed, the existence of only one

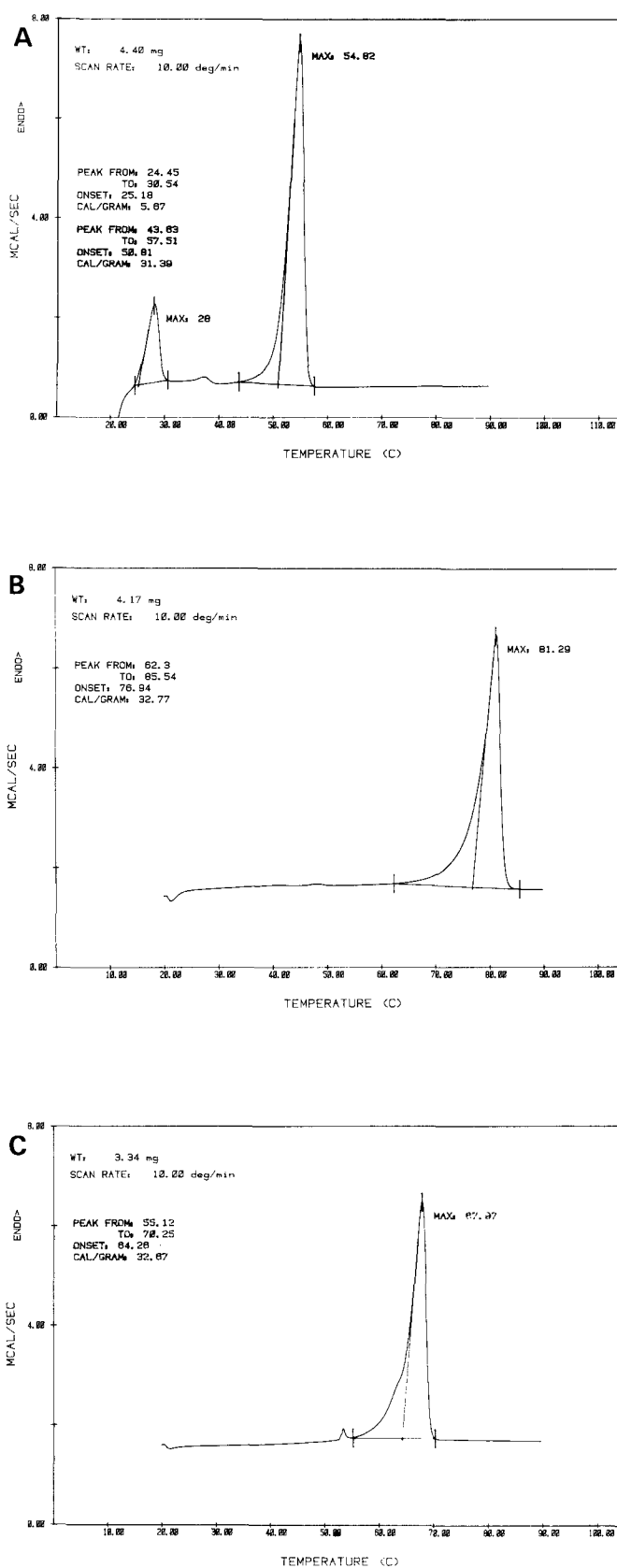


FIG. 8. DSC curves for anhydrous samples containing (A) 100% FA mixture; (B) 50% Stedbac and 50% FA mixture; (C) 100% Stedbac.



peak in the 50/50 sample and the increase in enthalpy of this low temperature peak with increasing Stedbac concentration indicate, when combined with the microscopy results described previously, that the fibrous crystals described above melt at about 55 C and the FA-rich particles at about 62 C. It is possible that equilibrium is not maintained during heating in some of these experiments because of the short equilibration times relative to those used in the PLS and microscopy studies.

*Temperature effects on phase behavior by microscopy.* Behavior of selected samples was observed as a function of temperature using hot stage microscopy. Observations made with two samples are of primary interest. One sample had a high FA-to-Stedbac ratio and exhibited the network structure involving particle-rich and fibrous regions discussed previously. The other

with less FA and more Stedbac contained many fibrous crystals but very few particles.

Figure 10A, taken with crossed polarizers, shows the structure at 35.7 C of a sample containing 0.6% Stedbac and 6% of the FA mixture. In registration with this view but with a  $1/4 \lambda$  plate at  $45^\circ$  relative to the polarizers is Figure 10B, in which the network of particle-rich regions is readily visible. Also noteworthy is that the periphery of the large particles is not smooth but exhibits some "corners." Presumably, the same is true for the small particles. The basic network can also be discerned from Figure 10A upon recognizing that Maltese crosses are the characteristic birefringent pattern produced by the particles, whereas the rather fuzzy, bright patches emanate from fibrous regions. Without this knowledge, however, identification of the network would be difficult using only the image taken with crossed polarizers (Fig. 10A). Use of other microscopy techniques, especially modulation contrast optics, has not only allowed us to see the network clearly but also demonstrated the existence of fibrous and particle containing regions.

The corresponding view (still in registration) with crossed polarizers +  $1/4 \lambda$  plate but at a temperature of 58.4 C is shown in Figure 11. The network structure seems basically the same as at the lower temperature, but it appears to have become less distinct.

Upon further heating the birefringence disappears completely at a temperature near 60 C. As the DSC results indicate, melting of the solid phases is complete at about this temperature.

When Stedbac and FA contents are 2.0% and 1.4% by weight, fibrous regions are seen at room temperature, as shown in Figure 12. The overall appearance is, as might be expected, similar to that shown in Figure 7 for a sample with slightly lower Stedbac content. An interesting structural feature is the bright region at the center of Figure 12. It resembles a cluster of small particles but was found on careful examination of the sample by focusing at various depths to actually be the ends of many closely-packed fibers which are oriented perpendicular to the plane of the photograph but bend into the plane at some depth.

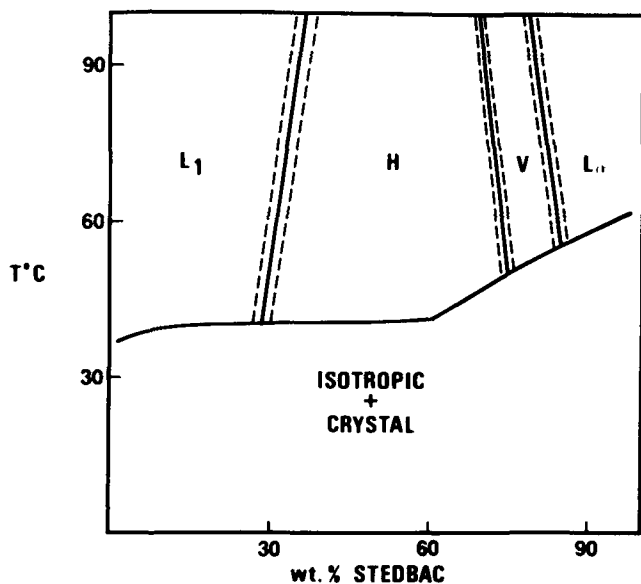


FIG. 9. Stedbac-H<sub>2</sub>O phase diagram. L<sub>1</sub>, Micellar solution; H, hexagonal; V, viscous isotropic cubic; L<sub>2</sub>, lamellar phases.

TABLE 2  
Aqueous Fatty Alcohol-Stedbac Dispersions

Wt % FA	Wt % Stedbac	Endotherms [onset temp, °C (enthalpy, cal/g solids)]		
		T <sub>1</sub>	T <sub>2</sub>	T <sub>3</sub>
A. 50% Water				
90	10	18 ( 4)		64 (31)
67	33	—		67 (21)
50	60	—		74 (31)
0	100		40	
B. 93.4% Water (1st heating)				
91	9	57 (10)		62 (20)
50	50	56 (18)		—
C. 93.4% Water (Repeat heating)				
91	9	55 (5)		63 (26)

## PHASE BEHAVIOR AND NETWORK FORMATION

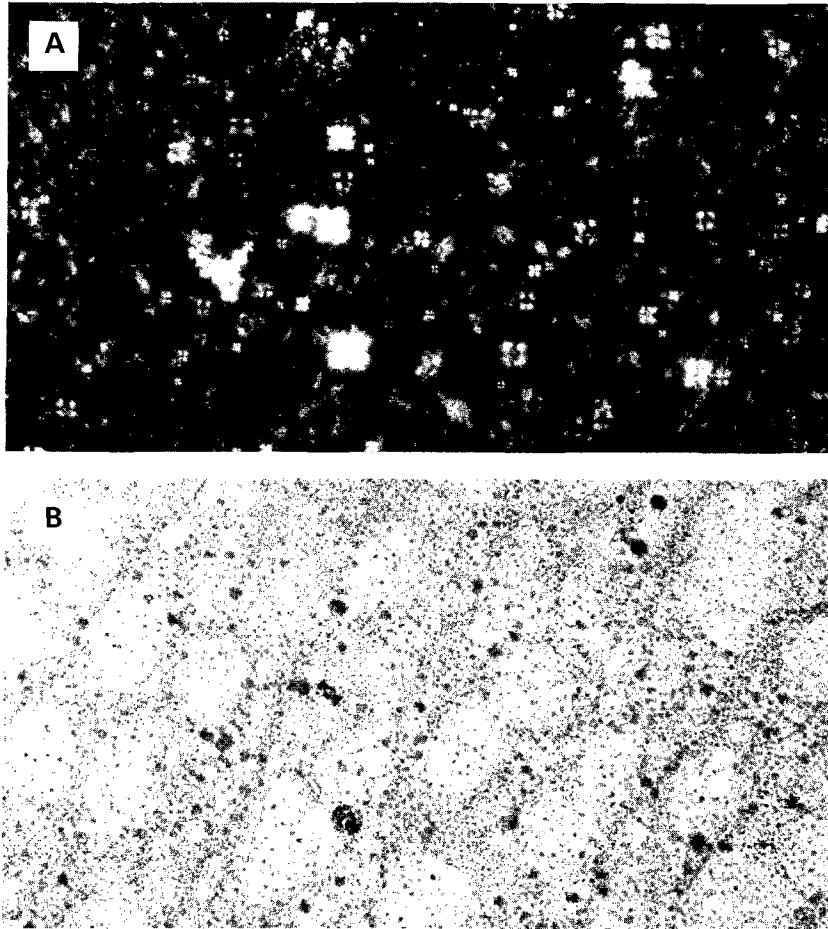


FIG. 10. Photomicrograph of 0.6% Stedbac and 6.0% FA mix.  $\times 181$ . Temp = 35.7 C. (A) polarized light; (B) same +  $1/4\lambda$ .

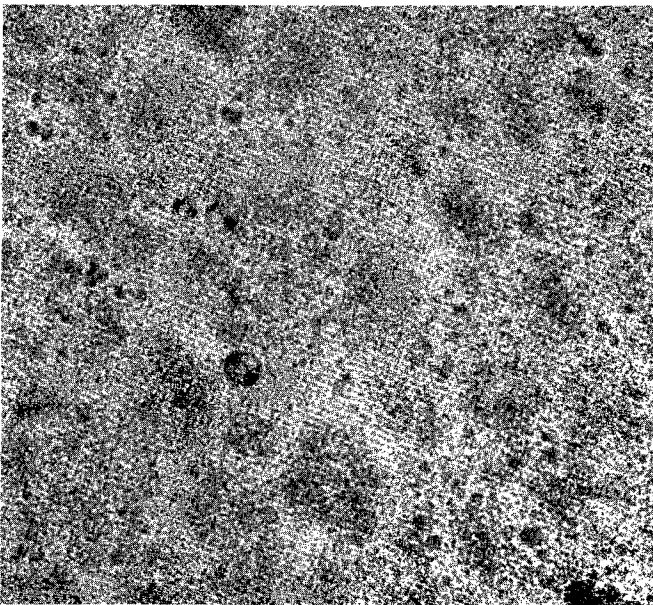


FIG. 11. Photomicrograph of 0.6% Stedbac and 6.0% FA mix. Polarized light +  $1/4\lambda$ .  $\times 181$ . Temp = 58.4 C.

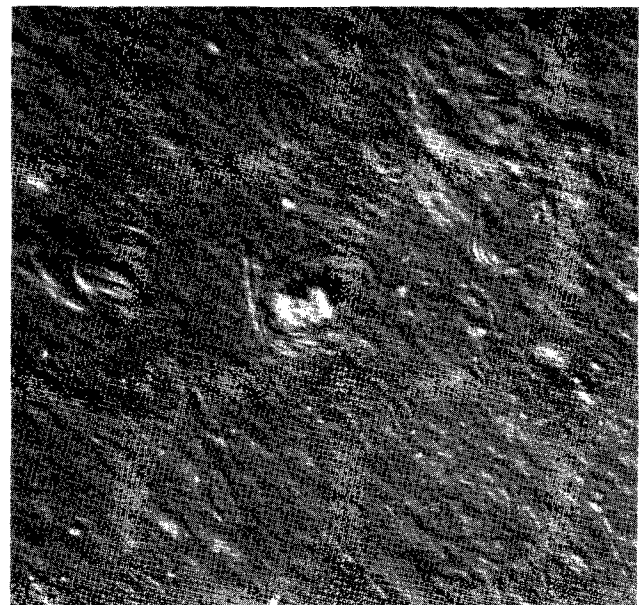


FIG. 12. Photomicrograph of 1.4% Stedbac and 2.0% FA mix. Modulation contrast  $\times 723$ .



When this sample was heated to 66.5 C, all birefringence disappeared, and drops of a liquid phase immiscible with water were seen. When it was cooled to 60 C and maintained at that temperature for five hr, both individual drops and clusters of drops were found.

Further cooling to 48.8 C caused crystallization of fibers, mostly as more or less spherical clumps, as shown in Figure 13A, taken with crossed polarizers, and Figure 13B, in registration with Figure 13A and with the  $1/4 \lambda$  plate also inserted. Note that several of the clumps appear to be interconnected, an illustration of a possible method for network formation in samples containing mostly fibers. No further changes in structure were found upon further cooling to 30 C.

We emphasize that for both these samples, as well as for others not discussed here in detail, observable changes in the initial structure did not occur until the temperature exceeded 55 C, i.e., until the melting temperature was approached. In particular, no changes were seen between room temperature and about 49 C, even when temperatures near the latter value were maintained for periods of up to 24 hr.

## DISCUSSION

The observations described above clearly indicate that two types of colloidal material are present in these

systems. One type has a generally spherical appearance (although the actual shape may be disk-like, as indicated above), exhibits Maltese crosses when viewed with crossed polarizers, and becomes more prevalent when the alcohol-to-surfactant ratio is increased. Such particles may consist of alcohol-rich lamellar liquid crystal, or, more likely, in view of the corners seen along their outer edges, a "gel" phase in which the hydrocarbon chains of a lamellar phase are in a frozen state instead of the liquid-like state characteristic of liquid crystalline phases. Particles with corners made up of such a phase have been observed in another system (22 and Benton, W.J., unpublished results).

The other colloidal material consists of small crystalline acicular or needle-like fibers which clearly contain more surfactant than the spherical particles since they become predominant with decreasing values of FA-to-Stedbac ratio. Some information about their composition may be gained from the observation that virtually no FA-rich particles are seen when the FA-to-Stedbac ratio is less than about 1.5 by weight. Thus, the composition of the fibers apparently does not differ greatly from that of the crystalline complex formed in anhydrous systems.

Groups of fibers clearly have a strong tendency to become aligned and pack together, forming the fibrous regions described previously. Such a tendency is

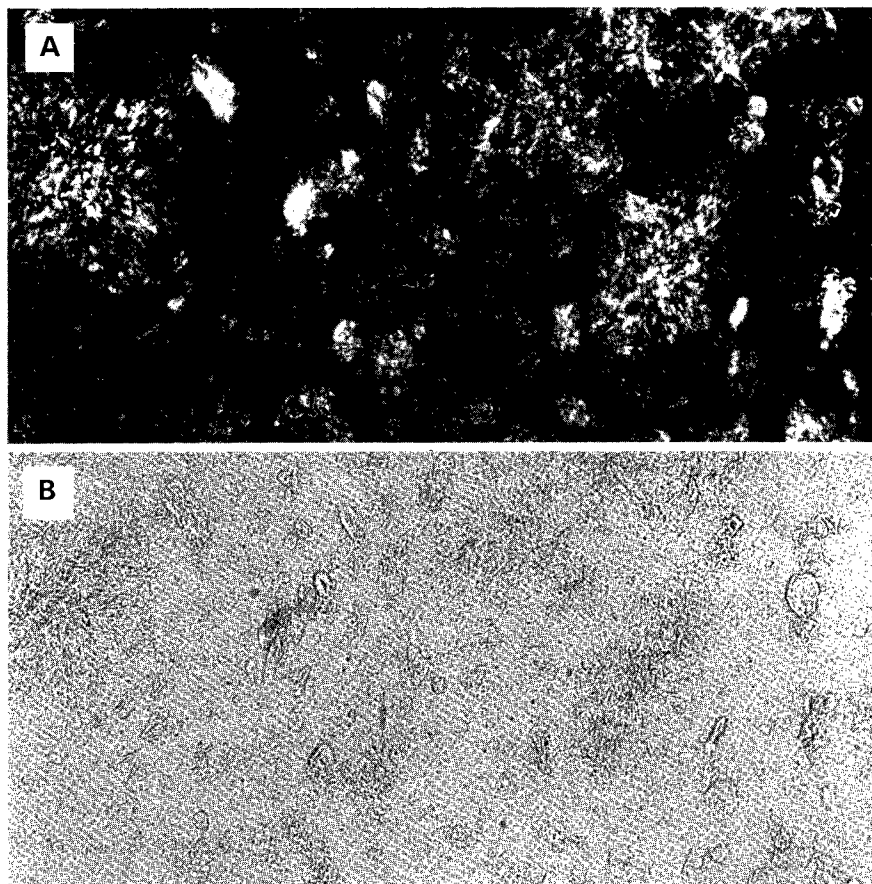


FIG. 13. Photomicrograph of 1.4% Stedbac and 2.0% FA mix.  $\times 181$ . Temp = 48.8 C. (A) polarized light; (B) same +  $1/4\lambda$ .

expected for such highly anisotropic particles and has been observed for the rod-like tobacco mosaic virus and analyzed theoretically by Onsager (23). Theoretical calculations show that separation of a phase of aligned rods is caused by an entropy effect and takes place even when there is no attractive interaction between rods (although with attraction phase separation occurs more readily). Moreover, separation can occur at very small volume fractions of particles when the aspect ratio, i.e., ratio of length to diameter, is large. For example, if the aspect ratio is 50, phase separation begins at a volume fraction of about 0.05 (24). A similar effect occurs for anisotropic particles having the shape of disks.

Since the fibers contain a substantial proportion of surfactant molecules, they presumably are positively charged. To a first approximation, electrical repulsion can be included in Onsager's analysis of phase separation by taking an effective radius of the fiber equal to its actual radius plus a length comparable to the thickness of the electrical double layer, which is a measure of the range of significant repulsion (22,23). This so-called Debye length is about 3 nm in these salt-free systems. Hence, the fibrous regions may contain appreciable quantities of water.

What seems to happen in the present system is that a mixture of the two colloids forms upon cooling a sample from above about 70 C, the relative amounts of the two depending on system composition. The FA-rich particles form first. Then fibrous regions develop in accordance with the above separation mechanism, excluding most particles which disrupt local fiber alignment. If many particles are present, as is the case at high FA-to-Stedbac ratios, the remaining portion of the sample becomes a concentrated colloidal suspension of particles and a network structure develops as described above (Fig. 3). The more disklike the particles, the more they too favor separation into distinct particulate and fibrous regions. The fine structure of the particulate region could not be seen clearly with the modulation contrast objectives presently available. Thus, we cannot say whether the particles are arranged in chains as reported by Gstirner et al. (9) based on electron microscopy studies in a related system.

If few particles are present, as seen at lower alcohol-to-surfactant ratios, the fibrous regions may still aggregate to form a network. As indicated above it would seem that such a network would be more susceptible to structural breakdown and syneresis than that found in the systems with higher alcohol content.

The behavior shown in Figure 2 can now be explained qualitatively. At low Stedbac concentrations (below about 0.3 wt %), many particles and few fibers are formed. Since the FA-rich particles are not strongly charged electrically, they flocculate and separate from

the water. As Stedbac concentration is increased, the amounts of particulate and fibrous material become comparable, and a network structure exhibiting both particulate and fibrous regions is seen which stabilizes the system, preventing macroscopic separation.

With further increases in Stedbac concentration, fibrous regions predominate. They may occupy the entire sample as occurs at the higher solid contents, or they may form a network having cells or channels of water. Finally, addition of still more Stedbac leads, at low FA concentrations, to macroscopic phase separation. In this case, separation occurs between a colloidal dispersion, which presumably contains fibers, and an aqueous solution.

## REFERENCES

1. *Micellization, Solubilization, and Microemulsions*, Vols. 1 and 2, edited by K.L. Mittal, Plenum, New York, 1977.
2. *Solution Chemistry of Surfactants*, Vols. 1 and 2, edited by K.L. Mittal, Plenum, New York, 1979.
3. Ekwall, P., *Adv. Liq. Cryst. 1:1* (1975).
4. Tiddy, G.J.T., *Phys. Reports 57:1* (1980).
5. Barry, B.W., *Rheol. Acta 10:96* (1971).
6. Barry, B.W., and G.M. Saunders, *J. Colloid Interface Sci. 34:300* (1970).
7. Barry, B.W., and G.M. Saunders, *J. Texture Studies 4:53* (1973).
8. Eccleston, G.N., *Cosmetics and Toiletries 92:21* (1977).
9. Gstirner, R., D. Kottenberg and A. Maas, *Arch. Pharm. 302:340* (1969).
10. Overbeek, J.T.G., in *Colloid Science*, Vol. 1, edited by H.R. Kruyt, Elsevier, Amsterdam, 1952, p. 368.
11. Overbeek, J.T.G., in *Colloidal Dispersions*, edited by J.W. Goodwin, Royal Society of Chemistry, London, 1982, pp. 16-17.
12. Miller, C.A., and D.D. Miller, *Colloids and Surfaces 16:219* (1985).
13. Fukushima, S., M. Yamaguchi and F. Harusawa, *J. Colloid Interface Sci. 59:159* (1977).
14. Laughlin, R.G., *Ibid. 55:239* (1976).
15. Benton, W.J., and C.A. Miller, *J. Phys. Chem. 87:4981* (1983).
16. Benton, W.J., E.W. Toor, C.A. Miller and T. Fort Jr., *J. Physique 40:107* (1979).
17. Hoffman, R., and L. Gross, *Appl. Optics 14:1169* (1975).
18. Benton, W.J., and C.A. Miller, *Prog. Colloid Polymer Sci. 68:71* (1983).
19. Miller, C.A., S. Mukherjee, W.J. Benton, J. Natoli, S. Qutubuddin and T. Fort Jr., in *Interfacial Phenomena in Enhanced Oil Recovery*, edited by D.T. Wasan and A.C. Payatakes, AIChE Symp. Ser. 212(78), 1982, pp. 28 ff.
20. Zasadzinski, J.A., L.E. Scriven and H.T. Davis, *Phil. Mag. A 51:287* (1985).
21. Kolp, D.G., and E.S. Lutton, *J. Chem. Eng. Data 7:207* (1962).
22. Evans, D.F., E.W. Kaler and W.J. Benton, *J. Phys. Chem. 87:533* (1983).
23. Onsager, L., *Ann. N.Y. Acad. Sci. 51:627* (1949).
24. Forsyth, P.A., S. Marcelja, D.J. Mitchell and B.W. Ninham, *Adv. Colloid Interface Sci. 9:37* (1978).

[Received April 22, 1986]